Early stages of cesium adsorption on the As-rich $c(2\times8)$ reconstruction of GaAs(001): Adsorption sites and Cs-induced chemical bonds

C. Hogan,[1] D. Paget,[2] Y. Garreau,[3] M. Sauvage,[3] G. Onida,[4] L. Reining,[5] P. Chiaradia,[1] and V. Corradini[6]
[1]*Dipartimento di Fisica and INFM, Università di Roma "Tor Vergata," 00133 Roma, Italy*
[2]*Laboratoire de Physique de la Matière Condensée, Ecole Polytechnique, 91128 Palaiseau cedex, France*
[3]*LURE, CNRS-MR-CEA, Bâtiment 209d, Centre Universitaire Paris-sud, BP34, 91898 Orsay, France*
[4]*Dipartimento di Fisica and INFM, Università di Milano, Italy*
[5]*Laboratoire des Solides Irradiés, UMR 7642 CNRS/CEA, Ecole Polytechnique, 91128 Palaiseau cedex, France*
[6]*Dipartimento di Fisica and INFM, Università di Modena, 1 Via G. Campi, 213/A I-41100, Modena, Italy*
(Received 4 June 2003; published 19 November 2003)

We investigate the adsorption of Cs on the As-rich $c(2\times8)/(2\times4)$ reconstruction of GaAs(001) at low coverages using a combination of theoretical and experimental techniques. Density-functional-theory local-density-approximation total-energy calculations and x-ray diffraction experiments find only minimal Cs-induced surface relaxation and identify three preferential adsorption sites within the partially disordered overlayer. These sites are, in order of decreasing occupation probability, the arsenic dimer bridge *D* site, the gallium dangling bond T_2' site, and the arsenic T_3 trench site. Detailed analysis of the wave functions and electronic charge densities allows us to clarify the bonding mechanisms at the three sites. At the gallium site, the bonding is strongly ionic and involves significant charge transfer to a new Cs-induced state reminiscent of the p_z orbital of the gallium atom in the sp^2 configuration. In sharp contrast, at the arsenic sites, the charge transfer is minimal and the bonding rather occurs through mixing with a relatively delocalized state of the clean surface. The ionization energy decreases are estimated and compared for the three sites.

DOI: 10.1103/PhysRevB.68.205313 PACS number(s): 78.40.Fy, 78.68.+m, 73.20.At

I. INTRODUCTION

The interaction between alkali atoms and semiconductor surfaces has long been the object of intensive fundamental studies, because of technological applications related to the lowering of the surface work function and because the absence of chemical reactions at the interface makes it a model system. From an experimental point of view, such studies have mostly concerned GaAs and silicon, using Auger spectroscopy and low-energy electron diffraction,[1–3] core level spectroscopy,[4,5] electron loss spectroscopy,[6,7] scanning tunneling spectroscopy,[8] and x-ray diffraction.[9–11] *Ab initio* calculations have been performed using Na adsorption on GaAs(110),[12] Cs adsorption on GaAs clusters simulating the (110) surface,[13] and K adsorption on Si(001).[14]

Among all these studies, only a very small fraction have considered very-low-coverage conditions, for which the alkali-alkali interactions are negligible as compared with alkali-substrate interactions. In this regime, fundamental aspects of the latter interactions can be investigated in detail. In order to investigate the adsorption on a microscopic scale, it is first desirable to identify the adsorption sites and to evaluate the displacement of substrate atoms induced by adsorption. It is of further interest to characterize the nature of the chemical bond between the adatom and the surface, to determine the amount of charge transfer between the electropositive alkali and the solid, and to analyze the nature of the alkali-induced surface dipole. For (001) and (011) surfaces of III-V semiconductors such as GaAs, one may think that, due to the presence of cations and anions at the surface, alkali atoms should preferentially adsorb near the empty dangling bonds of cation sites. This has been predicted using a reasoning based on a tight-binding treatment of the hybridization of the outer *s* electron of the alkali and of the surface dangling bond.[15] For Cs adsorption at the (110) cleavage face, using scanning tunneling microscopy (STM),[16] it has indeed been found that, at very low coverage, Cs atoms adsorb near Ga atoms. Calculations of adsorption of Na at the same surface[12] have shown that adsorption does not induce a breaking of surface chemical bonds, but results in a derelaxation of substrate atoms. The bonding between Na adatoms and substrate gallium atoms occurs through hybridization of the outer *s* alkali state and of the empty gallium dangling bond. The alkali *s* electron is partially transferred into the Ga dangling bonds, with only a weak perturbation of the latter. This transfer produces a surface dipole which, together with the alkali-induced change of surface dipole caused by the substrate derelaxation, explains the lowering of the ionization energy.

For adsorption at the (2×1) reconstruction of the (001) surface of Si, the situation seems to be quite different. Using x-ray diffraction,[10] it was found that the dimer site *D* and the trench site T_3 are jointly populated, thus creating some disorder in the alkali overlayer. For the former site, the silicon dimer bond seems to be broken, with a Si-Si distance close to its bulk value. These results are at variance with the ones found on the similar surface of germanium,[9] for which the Ge-Ge distances do not change by more than 8%, and in particular, the Ge dimer bonding length is essentially unchanged. Calculations performed for the K/Si system[14] conclude that, at low coverage, the adatom region remains neutral, so that the amount of charge transfer is limited. The surface dipole originates from a polarization of the adatom due to the Si-K mixing. The same conclusion is also reached by a core level investigation for the same system.[17]

In general, other bonding mechanisms may occur. At the very initial stage of Cs adsorption on *p*-type GaAs, the surface barrier increase has been interpreted as being caused by a charge transfer to the valence band of the bulk crystal.[18] For further adsorption, the surface Fermi level becomes pinned by Cs-induced states so that possible transfer processes are limited to the near-surface region. Another bonding mechanism consists in an ionic bonding by transfer of charge to a near-surface state induced by the presence of the adsorbed Cs atom. Such states have been predicted by Heine.[19]

In the present paper, we consider adsorption of Cs on the arsenic-rich $c(2\times8)$ reconstruction, for which the geometrical and electronic properties are well known, owing, respectively, to x-ray diffraction,[20] STM,[21] and *ab initio* calculations.[22] The geometry of adsorption, which is so far almost completely unknown, is investigated using both *ab initio* calculations and x-ray diffraction. Based on the combined experimental and theoretical results, we outline three dominant adsorption sites: the top dimer site D; the T_2' site, which is near the empty gallium dangling bond; and, to some minor extent, the T_3 trench site. The joint population of these sites is in agreement with previous findings, according to which it has been proposed that the Cs adsorbate is disordered based on low-energy electron diffraction (LEED) (Ref. 23) and STM (Ref. 24) measurements, whereas tight-binding calculations predict the existence of preferential sites for potassium adsorption.[25] We find that cesium adsorption has a very small effect on the position of substrate atoms and, in particular, does not induce any dimer breaking.

Ab initio calculations are used to investigate the nature of the bonding at each of these sites. We find that the bonding mechanism, dipole formation, and charge transfer are different for the Ga site and for the As sites, which represent two extreme bonding schemes on the same surface that are dependent on the adsorption site. For adsorption at T_2', the $6s$ electron of the alkali is predominantly transferred to a new Cs-induced state and the bond is strongly ionic. In sharp contrast, for the As-related sites, the charge transfer is significantly smaller and the bonding instead involves hybridization with states of the clean surface. Also discussed are site-dependent reduction of the ionization energy and Cs-induced modifications of surface electronic states. These modifications will be confirmed by an analysis of the changes in surface optical anisotropy.[26]

The structure of the paper is as follows: Section II is dedicated to an *ab initio* study of the geometrical properties of the interface. In Sec. III we experimentally confirm the above predictions using x-ray diffraction. In Sec. IV we analyze the nature of the chemical bond between Cs and the surface. Overall conclusions are presented in Sec. V.

II. THEORY

A. Computational method

Total-energy calculations of Cs adsorption were performed within the first-principles density functional-theory local-density-approximation (DFT-LDA) framework with the molecular-dynamics Car-Parrinello method. The theoretical equilibrium value for the lattice constant, $a_0=5.58$ Å, was used. Norm-conserving pseudopotentials (NCPP's) were adopted for all atomic species, and nonlinear core corrections[27] (NLCC's) were used with gallium. For the Cs atom, the NCPP was constructed with special care, treating the whole fifth electronic shell as valence, together with the optical $6s$ electron. This choice for partitioning core and valence electrons avoids the problems encountered when the fifth shell, which is highly polarizable, is treated as part of the core.[28] Restricting the core up to only the fourth shell meant having a slower convergence with respect to the number of plane waves required in calculations, due to the steeper character of the pseudopotential. We hence chose to work with modern norm-conserving pseudopotentials of the class introduced by Hamann,[29] which avoid the additional complications of the Vanderbilt[30] non-normconserving pseudopotentials and, at the same time, allow the use of a reasonably small number of plane waves [remarkably lower than with a traditional NCPP (Ref. 31)]. By carefully choosing the core radii (1.2 bohr for the *s* component, 1.4 bohr for the *p* component; all higher-l components were assumed to be equal to the *s* one), we obtained a pseudopotential for Cs which combines a relatively fast convergence (12 Ry already give a satisfactory convergence) with excellent transferability. The latter was tested not only through the behavior of the logarithmic derivatives, but also by explicit calculations of the Kohn-Sham eigenvalues for some excited atomic configurations against the corresponding all-electron results. Furthermore, we performed some convergence tests using Cs_2 clusters inside periodically repeated supercells. The results, shown in Table I, demonstrate that a cutoff of 13 Ry gives well-converged structural and energetic properties. We note that Cs pseudopotentials with nine valence electrons have been reported elsewhere to give the best results in Cs_2 studies.[32]

TABLE I. Convergence tests of the Cs pseudopotential using Cs_2 clusters. Shown, as a function of the kinetic energy cutoff, Cs-Cs bond length d, cohesion energy E_{coh}, and LDA band gaps (calculated for $d=4.76$ Å).

Cutoff (Ry)	d (Å)	E_{coh} (eV/atom)	E_{gap} (eV)
8	4.955	0.5412	0.87
11	4.805	0.5397	0.96
13	4.741	0.5380	1.04
30	4.735	0.5374	1.04

Following previous results,[20–22] we considered a β_2 unit cell, which is depicted in Fig. 1. This structure consists of two As dimers at the top layer with a further As dimer situated at the third atomic layer. Possible alkali adsorption sites, also indicated in the figure, are labeled D and D' for dimer sites and T_n and T_n' for trench sites on an atom belonging to the nth atomic layer. The surface was simulated with periodically repeating supercells of thin GaAs slabs separated by vacuum regions. Gallium dangling bonds on the back surface were saturated with a layer of fractionally charged ($Z=1.25$) hydrogen like pseudoatoms. Initial geometrical optimization and identification of favorable adsorption sites was

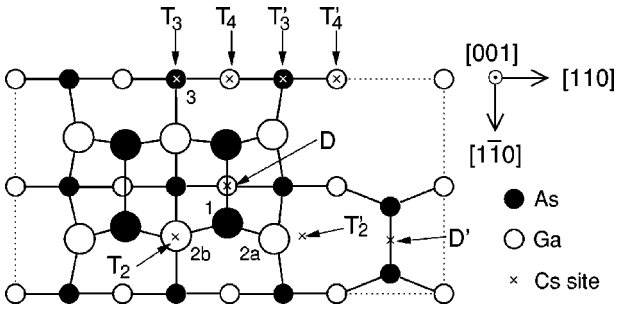

FIG. 1. Top view of the unit cell of the $\beta_2(2\times4)$ reconstruction of GaAs(001). Shown in the figure are several possible adsorption sites for cesium: trench sites situated over atoms of the nth layer are labeled T_n, whereas D and D' denote dimer bridge sites. Selected atoms are also labeled.

carried out with a kinetic energy cutoff of 11 Ry and supercells consisting of six atomic layers and 8 Å of vacuum. For the computation of total energies the ground states were recalculated at 13 Ry using thicker slabs of ten atomic layers and 10 Å of vacuum. All trends with respect to the adsorption sites (i.e., total-energy differences, spectral modifications) were consistent between the thick and thin slabs. A single **k** point (Γ) was used during the surface optimization, in which the bottom two layers were fixed to the ideal bulk positions and all other atoms were allowed to relax until the atomic forces did not exceed 35 meV/Å.

B. Geometry of adsorption: Results

Geometry optimization was carried out on the alkali-metal/semiconductor slab for several initial positions of a single Cs atom adsorbed on the β_2-reconstructed (2×4) surface. Sites in the "missing dimer" region—i.e., in the lower plateau region near D'—are not favored, as all our attempts to find relatively stable adsorption sites there were unsuccessful. We found two independent, energetically favorable adsorption sites—namely, the symmetric T_3 site and the D site—which were previously identified as the more stable for cesium adsorption on Si(100).[10] We also identified the T_2' site, close to the Ga empty dangling bond, as a stable adsorption site. As expected,[33] the adsorption energies are slightly higher than those found for Na on GaAs(110), which are of the order of 1.2–1.8 eV.[12] Among the three investigated sites T_3 has the highest adsorption energy of 2.42 eV, while the D and T_2' sites are lower, by 0.38 eV and 0.56 eV, respectively.

An important point to note is that the Cs-induced relaxation of substrate atoms is, in general, negligible. Breaking of dimers is not found to occur for any configuration. For adsorption at the D and T_3 sites, the largest atomic displacements, which involve the top layer dimers, are of the order of 0.05 Å and correspond to a fraction of the order of 10^{-3} of the unit cell dimension. The dimer length is calculated to be 2.42 Å, which is very close to the value for the clean surface, 2.44 Å. For the T_2' structure, the dimer length is slightly lower, at 2.40 Å. The nearby Ga atom is found to move inwards by 0.23 Å, corresponding to a vertical displacement of 16% of the spacing between atomic planes. This behavior mirrors the reported partial derelaxation of the GaAs(110) surface[12] under low coverage of Na, in which the Ga atom nearest to the alkali moves by $\approx$0.36 Å, while other atoms are mostly unaffected.

III. SURFACE X-RAY DIFFRACTION

A. Experiment

Surface x-ray diffraction studies of the Cs adsorption, performed at the DCI storage ring of Lure, Orsay, allow us to verify the predictions of the calculation. The surface was prepared *in situ* by molecular beam epitaxy using successive evaporations of Ga and As at 600 °C, until a sharp reflection high-energy electron diffraction (RHEED) pattern was observed. The sample was then slowly cooled to room temperature, which did not result in a significant change of the RHEED pattern and was transferred and aligned in the x-ray diffractometer. Alkali adsorption was performed using thoroughly outgassed SAES getters. The x-ray diffraction pattern was referred to a 2×4 surface basis related to the bulk fcc unit vectors by

$$\mathbf{a}=[1\bar{1}0]_{\text{cubic}},\quad \mathbf{b}=2[110]_{\text{cubic}},\quad \mathbf{c}=\frac{1}{2}[001]_{\text{cubic}}. \quad (1)$$

The reconstruction of the starting surface was $c(2\times8)$, for which the unit cell is known to be composed of (2×4) patterns.[20] The relative intensities of the diffraction spots were completely identical to those already published elsewhere for the β_2 surface.[20] As found from the analysis of their Lorentzian widths, the surface quality was very good, and the coherence length was found to be of the order of 300 Å.

A preliminary qualitative investigation of Cs adsorption was performed. No sign of surface disorder could be found after alkali atom adsorption, since the Lorentzian linewidth stayed constant, and no increase of the background signal could be observed. These results are at variance with the observed strong degradation of the LEED pattern observed on the same surface.[23,34] These differences can be understood if we assume the presence of a limited disorder among the Cs overlayer: the highly surface-sensitive LEED pattern reflects the partially disordered overlayer, whereas due to its increased penetration depth, x-ray diffraction is more sensitive to the underlying reconstructed surface. It should be noted that the minimum escape depth of electrons in Cs is particularly low, about 2.5 Å.[35] Because the coherence length is at least one order of magnitude larger for x rays than for low-energy electrons, the quality of the x-ray diffraction pattern, which depends on the number of coherent scatterers—i.e., on the square of the coherence length—should also be significantly better than that of the LEED pattern.

We find that Cs adsorption induces significant changes in the intensities of diffraction spots. Shown in Fig. 2 are, as an example, the results obtained for the diffraction spots defined by their position in reciprocal space, $(h,k,l)=(4,5,0.05)$ and $(h,k,l)=(4,7,0.05)$. These intensities exhibit strong changes up to 50 min adsorption. At the initial stage, the intensity of the (4,7,0.05) diffraction spot increases up to approximately 10 min exposure, stays constant up to 20 min exposure, and

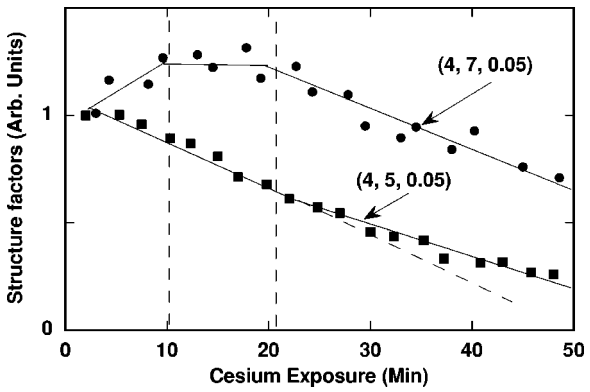

FIG. 2. Variation of two selected structure factors measured during cesium adsorption. The solid and dotted lines are guides to the eye.

starts to decrease for further Cs adsorption. In the same conditions, the intensity of the (4,5,0.05) diffraction spot decreases linearly up to 20 min and exhibits a change of slope for larger exposures. These characteristic phases are also found from the intensities of other diffraction spots (not shown here) and probably reflect distinct phases in the adsorption process. It is probable that these stages correspond to adsorption of one Cs per (2×4) unit cell after 10 min exposure and of a second one after a double exposure of 20 min. As a result, in order to verify the predictions of the *ab initio* calculation, we have chosen an evaporation delay of 9 min.

After adsorption, the intensities of 34 diffraction spots in the $l=0$ plane were measured. Ten of these structure factors showed a change larger than 50%. Also measured were five selected rods, defined as the diffracted intensity as a function of l for fixed values of h and k. Half-order diffraction spots in the h direction were diffuse and were not measured, so that no distinction can be made between the $c(2\times8)$ symmetry and a (2×4) one. The total number of independent data was 95.

B. Analysis

Analysis of the Cs-induced changes of the structure factors was performed using the ROD code[36] and consisted in choosing a starting atomic configuration and in allowing atomic motions in order to optimize a quality factor given by

$$\chi^2_{\mathrm{red}}=\frac{1}{N-p}\sum_{hkl}\frac{(F^{\mathrm{obs}}_{hkl}-F^{\mathrm{calc}}_{hkl})^2}{\sigma_{hkl}}, \qquad (2)$$

where N is the number of independent measured values and p is the number of adjustable parameters used in the fit, while F^{obs}_{hkl} and F^{calc}_{hkl} are, respectively, the experimental structure factors and their predicted values. The quantity σ_{hkl} usually corresponds with the experimental uncertainties and is generally taken to be 10% of the experimental structure factor. Here, in order to increase the sensitivity of the data to the Cs adsorption, we chose to decrease σ_{hkl} by one order of magnitude for the ten structure factors which exhibited the largest Cs-induced changes. The resulting sensitivity of χ^2_{red} to Cs adsorption can be estimated by comparing the experimental structure factors with their predicted values for the *clean* surface.[20] The agreement with the experimental data is quite poor, since we obtain a large value of χ^2_{red} of 268, which reveals a strong sensitivity to Cs and provides a reference value for χ^2_{red}.

TABLE II. Results, for several adsorption sites, of fitting to x-ray diffraction spectra. The quantity χ^2_{red} is defined in the text by Eq. (2), p is the number of adjustable parameters in the fit, and S is the optimum value of the site occupancy parameter.

Site	χ^2_{red}	p	S
D	4.4	21	1
T_2'	5.1	19	1
T_3	11.8	16	1
T_2	24	21	1
T_4'	29.8	22	1
D'	33	15	1
D	3.2	21	0.65

Due to the amount of surface disorder discussed above, a complete analysis of the changes would require the consideration of coadsorption at several distinct sites. However, since such analysis requires a prohibitively large number of adjustable parameters, we examined adsorption at only one site at a time. Some discrepancies are expected between the data and the fit, due to the sites which are neglected in the model. These discrepancies should be lowest for the most populated site so that a comparison of the results obtained for the various sites allowed us to determine the preferential site(s) and also to evaluate the Cs-induced relaxation of substrate atoms.

We considered all the sites shown in Fig. 1, taking as starting values the experimental atomic coordinates of the clean surface,[20] together with the calculated position of the Cs atom.[37] Initially we supposed that all cells are occupied by one Cs atom (occupation parameter S equal to unity). In Table II we present the values of χ^2_{red}, the number p of adjustable parameters, and the maximum occupancy factor S. As expected from the total energy calculations, we find that sites D, T_2', and T_3 lead to the best fits, while sites T_2, T_4, and D' lead to a relatively large value of χ^2_{red}. In a second stage, we progressively varied S, performing further adjustment of all the parameters. For the D site, the fit could be further improved by reducing S to 0.65 and gave the best value of χ^2_{red}, also shown in Table II. Shown in Fig. 3 are the experimental and calculated structure factors for the $l=0$ plane in the case of the D site. The agreement between the two sets of values is very good. Since the values of χ^2_{red} are artificially high due to the very low values for several σ_{hkl}, the quality of the fit was further characterized on an absolute basis by using the reliability factor $R=\Sigma_{hkl}(F^{\mathrm{obs}}_{hkl}-F^{\mathrm{calc}}_{hkl})^2/(F^{\mathrm{obs}}_{hkl})^2$. For these three sites R was found to range between values of 0.13 (for D) and 0.23 (for T_3). These values are low, such that, on the basis of the χ^2_{red} values, we

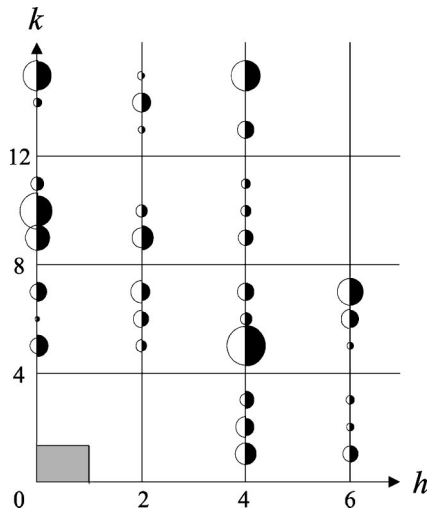

FIG. 3. Comparison between experimental in-plane structure factors (shaded semicircles) after 9 min cesium adsorption and their calculated values (open semicircles) for adsorption at the *D* site. The (1×1) reciprocal lattice is outlined by the square grid. The shaded rectangle at the origin displays the (2×4) unit cell.

infer that these three sites are probably jointly populated, with *D* being more populated than the other two sites.

Next, we consider the Cs-induced displacements of substrate atoms obtained in the fit. Most displacements were smaller than 10^{-2} of the unit cell, and the one or two values that exceeded this limit were smaller than 3×10^{-2}, a value slightly larger than that predicted by the *ab initio* calculations. These discrepancies are a direct consequence of the fact that we have considered adsorption at only one site at a time, so that the fitting procedure compensates for the absence of the other sites by using slightly unphysical atomic motions. Their values are, however, sufficiently small to discard any strong Cs-induced relaxation of the substrate (As dimer disruption requires a displacement larger than 10^{-1}). Finally, we considered the *out-of-plane* structure factors and obtained a fit, not shown here, which allowed us to interpret the general trends of the data, using the experimental atomic coordinates in the *xy* plane and the calculated *z* coordinates. The quality of the fit is approximately the same for *D* and T_2'.

In conclusion, the above analysis allows us to verify experimentally the predictions of the calculations: we find that the preferential adsorption sites are *D*, T_2', and T_3—namely, those identified in the *ab initio* calculations as having the largest adsorption energy. Furthermore, the Cs-induced atomic displacements are small, as predicted. The displacements are smaller than for adsorption at the similar Si(001) surface[10] and also at the GaAs cleavage face.[12] This latter finding is related to the fact that, as will be seen later, adsorption is found to involve interaction with several atomic layers, whereas on the cleavage face, adsorption mostly concerns the Ga dangling bonds. Table III summarizes the theoretical atomic coordinates of the Cs atom at the three sites considered here, in fractional units of the unit cell, taking as a reference the nearby As atom of the third layer. Atom labels are indicated in Fig. 1. The atomic displacements introduced by the fit, shown in parentheses, are small. Also given are several relevant distances between the Cs and the substrate atoms. The distance between the cesium atom and the neighboring gallium is found to be of the order of 3.8 Å. This distance is comparable with the distance of the Ga-Cs bond found in bulk compounds, which ranges between 3.75 Å and 3.85 Å depending on the configuration.[38] It is interesting that the trend in total energy with respect to the adsorption site inversely reflects the trend in $|$Cs-As$|$ length. Since both Cs and As have high electron concentrations in the outermost valence shells, it is likely that minimizing the electron repulsion competes with the energy gain from electron transfer in determining the most likely adsorption site.

Finally, note that the largest adsorption energy has been found for site T_3, which seems to be less populated than the two other sites, as seen from the larger value of χ^2_{red}. This difference suggests that the Cs adsorbate is not in thermody-

TABLE III. Atomic coordinates of Cs adsorption sites (T_3, *D*, T_2') and selected substrate atoms (1, 2*a*, 2*b*, 3; see Fig. 1), as used in the fitting of the x-ray diffraction data. Coordinates are shown with respect to As(3). $x||[1\bar{1}0]$ and $y||[110]$ are given in fractional units of the (2×4) cell vectors, while $z||[001]$ is given in fractional units of the fcc bulk cell constant (5.653 Å). Deviations $(\Delta x,\Delta y)$ from the Cs coordinates obtained during the fitting are noted in parentheses. These deviations are only nonzero for the T_2' site because of symmetry considerations. The fourth and fifth columns indicate the minimum Cs-As and Cs-Ga distances found in the *ab initio* calculations.

Atom	$x(+\Delta x)$	$y(+\Delta y)$	z	$\lvert$Cs-As$\rvert_{\min}$(Å)	$\lvert$Cs-Ga$\rvert_{\min}$(Å)
Clean surface					
As(1)	0.657	0.121	0.510		
Ga(2*a*)	0.732	0.211	0.199		
Ga(2*b*)	0.721	0.000	0.244		
As(3)	0.000	0.000	0.000		
Cesium surfaces					
Cs(T_3)	0.000	0.000	0.789	3.67 [As(3)]	3.73 [Ga(2b)]
Cs(*D*)	0.500	0.125	1.067	3.31 [As(1)]	5.39 [Ga(2a)]
Cs(T_2')	0.732 (+0.010)	0.287 (−0.017)	0.812	3.24 [As(1)]	3.84 [Ga(2a)]

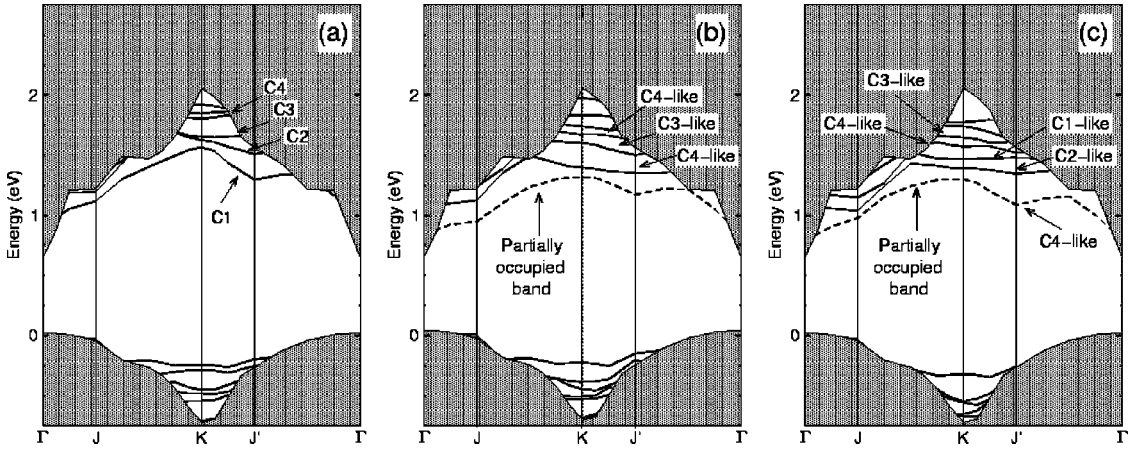

FIG. 4. Surface band structures of (a) clean, (b) Cs-covered (T_2' structure), and (c) Cs-covered (D structure) GaAs(001)$\beta_2(2\times4)$, plotted over the projected bulk band structure. The partially occupied band induced by the metal atom is indicated.

namic equilibrium and that the relative populations of these sites are determined by geometrical factors, such as the site density and the relative areas of the collection basins which lead to Cs adsorption at each of these sites. In comparison with the statistically unfavoured T_3 site (one site/cell), the fourfold T_2' sites and the two neighboring D sites which have a larger collection area should indeed be more populated.

IV. Cs/GaAs CHEMICAL BOND

A. Cs-induced states

Our discussion of the Cs/GaAs chemical bond begins with the computed band structures of the *clean* surface, shown in Fig. 4(a). The results agree with those published previously by Schmidt and Bechstedt[22]: surface states lie outside the fundamental gap (Γ point) and are concentrated around the K point of the surface Brillouin zone (SBZ). The reported underestimation of the band gap, a well-known feature of DFT-LDA, does not modify the physical picture to be described below. The four lowest-energy unoccupied states are labeled $C1-C4$, whereas states lying at higher energies will not be considered here, since they are weakly affected by adsorption, at least in their wave function character. In Fig. 5 we examine more closely the nature of the clean surface states via isosurface plots of the corresponding wave functions at the K point of the SBZ. The lowest two states ($C1$ and $C2$) are complementary states localized primarily at second-layer Ga orbitals, with a smaller contribution localized at the top layer dimers. $C2$ seems to correspond to the lowest unoccupied state found in Ref. 22. We note that four from six of the second-layer Ga atoms are threefold coordinated (sp^2 hybrid) to As; the remaining empty p_z-like orbitals are the most pronounced features in the figure. Both states feature a strong asymmetry in the $[1\bar{1}0]$ direction. More symmetric surface states are found localized at the third-layer As dimer ($C3$) and top-level dimers ($C4$), respectively.

Figures 4(b) and 4(c) show the calculated surface band-structure for adsorption at T_2' and D, respectively. The most notable Cs-induced change is the appearance of a *partially filled* band, shown by a dotted line in the figure, lying about a further 0.2 eV below the surface states of the clean surface.[39] This highest occupied state is responsible for the bonding between Cs and the surface. It is tempting to conclude that this state is also responsible for the known pinning of the surface Fermi level.[40] However, further work is necessary to reach this conclusion since the position of the band

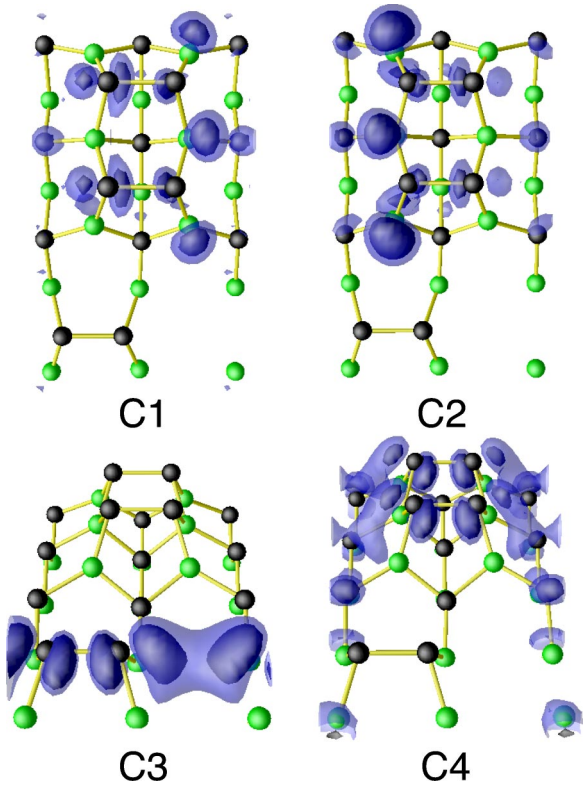

FIG. 5. (Color online) Isosurfaces of squared wave functions at K, for the four lowest unoccupied surface states of clean GaAs(001). Isosurfaces are plotted for $|\Psi|^2=0.0015$ bohr^{-3} and 0.0009 bohr^{-3}.

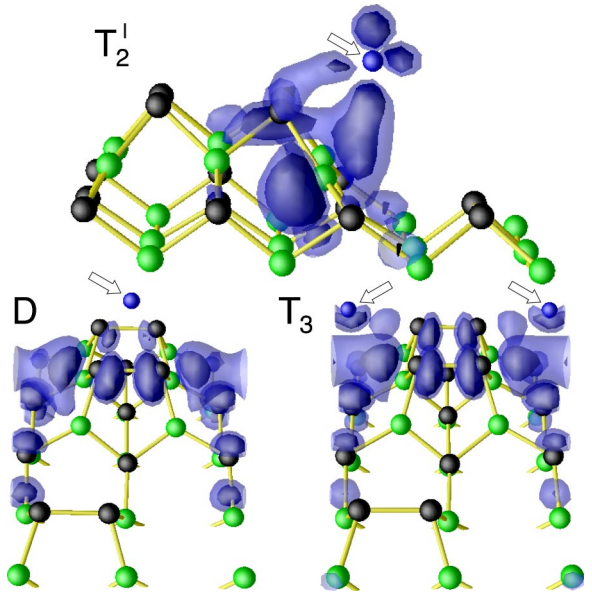

FIG. 6. (Color online) Same as Fig. 5, but for the highest occupied state on each of the cesium-covered surfaces. Isosurfaces are shown at 0.0030 bohr^{-3} and 0.0018 bohr^{-3} for the T_2' site, 0.0015 bohr^{-3} and 0.0009 bohr^{-3} otherwise. The Cs atomic position is indicated with an arrow in each case.

only approximately coincides with the experimental Fermi level position, determined to be near midgap, and since surface defects may also play a role, as has been suggested for the clean surface.[22,41] The valence state of the adatom mixes with the states $C1-C4$, which is expected since the Cs $6s$ atomic energy level (obtained from an identical supercell calculation for the free atom), is found to lie close in energy to the unoccupied surface states of the clean (001) surface (about 0.2 eV below $C1$ at the K point). However, examination of the wave functions, as compared to those of Fig. 5, shows that the nature of several states after adsorption is strongly reminiscent of that of states $C1-C4$, so that these states are labeled as C_i-like in Figs. 4(b) and 4(c).

For the T_2' site, inspection of Fig. 6 reveals that the partially occupied band at T_2' exhibits a significant density above the nearby Ga atom, as well as a stronger contribution *behind* this atom. Its isosurface is quite distinct from any of the above-described states of the clean surface, suggesting that Cs adsorption induces a *new* state. Similar induced states have also been found on GaAs(110) (Ref. 13) and even for adsorption on graphite.[42] The appearance of the latter state occurs at the expense of states $C1$ and $C2$ of the clean surface, which are no longer visible after adsorption. This picture can be understood using the shapes of the states of the clean surface: states $C1$ and $C2$ have a significant presence probability at the Ga dangling bond and therefore strongly interact with the Cs $6s$ state. They completely lose their character and are replaced by the new Cs-induced state. Other states are less modified and are still visible in the band structure. The strongest modification concerns the strongly symmetrical $C4$ state, which is split into two complementary bands localized on each of the top layer As dimers. The present picture of the bonding is in sharp contrast with that found in the case of Na adsorption at the cleavage face, in which molecular hybridization occurs between the outer s alkali state and states of the clean surface, mostly related to the empty Ga dangling bond. Qualitatively speaking, the Cs-induced T_2' bonding state is reminiscent of the p_z orbital of the sp^2-hybridized Ga atom, although we stress that it appears to be a new state, which does not exist on the clean surface. As we will see below, the latter is partially occupied by an electron coming from the Cs atom.

Although the Cs-induced band structure changes for adsorption at the arsenic D site are apparently quite similar to those found for T_2', analysis of the wave functions reveals, as expected, a very different bonding mechanism. The map of the partially occupied state, responsible for the bonding, is presented in Fig. 6 for the K point. This state is quite delocalized across the surface unit cell, with large contributions at the topmost As dimers, and hence is quite similar to $C4$. This strongly suggests that Cs adsorption, rather than introducing a new state as in the case of adsorption at T_2', hybridizes with $C4$ to form a pair of complementary states, the lowest-energy one being occupied in each case. Clearly, Ga orbitals do not play any significant role in the bonding since, after adsorption, states $C1-C3$ are still unoccupied and clearly identifiable. The fact that the Cs-induced modifications of surface states are significantly smaller than for the Ga site can be understood from simple considerations: state $C4$ should be weakly coupled to the nearby Cs state because the strongest contribution to the coupling should come from the charge clouds in the vicinity of each of the As atoms composing the dimer. These clouds are reminiscent of the antibonding state of the dimer and correspond to wave functions of opposite signs, so that their contributions to the interaction with the Cs state mostly cancel each other. Thus the coupling with the $C4$ state should be smaller than the one with $C1$ and $C2$ for Cs in the T_2' site. Adsorption at T_3 is quite similar to adsorption at D and will not be discussed here in detail. For this adsorption, the lowest two bands are $C4$ like and are followed by $C2$-like and $C3$-like bands. Due to the increased symmetry, the splitting of the $C4$ band, of 0.11 eV, is smaller than for the D site (0.27 eV at K).

B. Cs-induced dipoles

Using the above calculations, we now evaluate the lowering of the ionization energy. This lowering is determined in the same way as described in Ref. 12—i.e., from the Cs-induced change in the electrostatic potential. Since accurate calculation requires a well-converged electrostatic potential in the vacuum region, we performed further calculations[43] for clean and adsorbed surfaces using supercells with thicker vacuum regions of 16 Å. In addition, we used a dipole correction[44] within the vacuum region to remove the spurious macroscopic electric field that arises from the polar nature of Cs/GaAs(001) and, to a lesser extent, clean GaAs(001). The microscopic potential was first averaged in the plane of the surface before being passed through a filter[45] along z, of characteristic period $a_0/4$, in order to remove the usual oscillations between As and Ga planes. For the clean surface we obtain a value for the ionization energy of 5.64

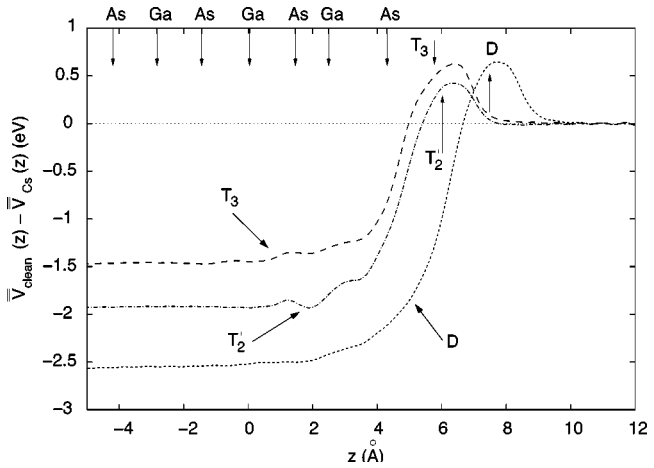

FIG. 7. Changes in macroscopic electrostatic potential $\overline{\overline{V}}$ of the relaxed GaAs(001) surface after adsorption of Cs at different sites. Vertical arrows denote atomic positions.

eV, in good agreement with the experimental value of 5.5 eV (Ref. 46) and with other calculations (5.61 eV, Ref. 47, and 5.43 eV, Ref. 22).

In Fig. 7 we present the resulting macroscopic potential changes for Cs adsorption at all three sites. We take as the origin of energy the vacuum level position, so that the change is zero in vacuum far from the surface. In the solid, we find a potential lowering which reveals the Cs-induced ionization energy decrease. The largest change, -2.6 eV, occurs for the D site, which is also the most populated one; the next largest change is -1.9 eV for T_2' while the smallest occurs for T_3 at about -1.5 eV. The positive bump in the potential difference, near the adatom centers, is characteristic of adsorption involving larger alkali atoms, as noted in Ref. 12, and reflects intra-atomic screening of the dipolar field. Accurate comparison of the ionization energy changes with the experimental ones is not straightforward since the experimental work function strongly depends on coverage, which cannot be determined precisely.[48] However, for the present case, using Ref. 2, we find that, for a coverage of 10%, the experimental work function change is approximately 1.6 eV. This value is in qualitative agreement with the above estimates, further taking into account the facts that experimental determination also includes surface barrier changes and that we have neglected interactions between dipoles.

We analyze the nature of the Cs-induced dipoles by considering the charge redistribution after adsorption. We have computed, as a function of spatial position $\mathbf{r}$, the charge difference $\Delta\rho(\mathbf{r})$ for adsorption at each site, defined by

TABLE IV. Average dipole charge $Q^{\pm}$, dipole length d_z, dipole moment p_z and change in electrostatic potential change as a function of adsorption site (see text).

Site	$\lvert Q^{\pm}\rvert(e)$	d_z (Å)	$p_z=\lvert Q^{\pm}\rvert\times d_z$	$\Delta\overline{\overline{V}}$ (eV)
D	2.17	+2.88	+6.24	2.6
T_2'	2.34	+2.60	+6.07	1.9
T_3	1.89	+1.10	+2.08	1.5

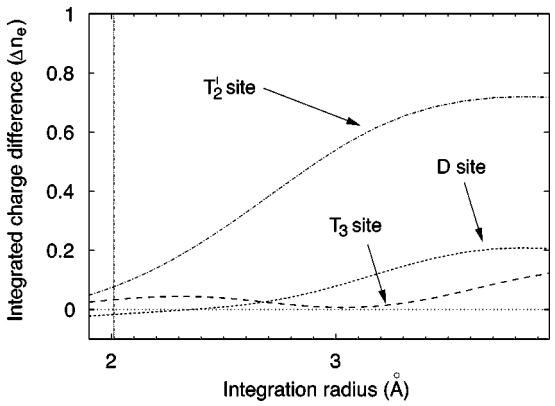

FIG. 8. Integrated Cs valence charge difference as a function of integration radius (see text), for the three adsorption sites.

$$\Delta\rho(\mathbf{r}) = \rho_{\mathrm{Cs}}(\mathbf{r}) + \rho_{\mathrm{GaAs}}(\mathbf{r}) - \rho_{\mathrm{Cs/GaAs}}(\mathbf{r}), \tag{3}$$

where $\rho_{\mathrm{Cs/GaAs}}$ is the total electron density (i.e., $\rho>0$) for the relaxed, Cs adsorbed slab, ρ_{GaAs} is that for the clean relaxed surface, and ρ_{Cs} is that for an isolated Cs atom (layer). In analogy to the center-of-mass concept, we calculate the quantities

$$Q^{+} = \sum_i \Delta\rho(\mathbf{r}_i) \quad \text{for } \Delta\rho(\mathbf{r}_i)>0, \tag{4}$$

$$Q^{-} = \sum_i \Delta\rho(\mathbf{r}_i) \quad \text{for } \Delta\rho(\mathbf{r}_i)<0, \tag{5}$$

$$d_z = \left.\frac{\sum_i \Delta\rho(\mathbf{r}_i) z}{Q^{+}}\right|_{\Delta\rho(\mathbf{r}_i)>0} - \left.\frac{\sum_i \Delta\rho(\mathbf{r}_i) z}{Q^{-}}\right|_{\Delta\rho(\mathbf{r}_i)<0}, \tag{6}$$

where the summations run over a mesh of points $\{\mathbf{r}_i\}$ describing the whole slab supercell. The quantities $Q^{\pm}$ and d_z represent, respectively, the average dipole charge and the average dipole length normal to the surface. Values for these quantities are given in Table IV, along with the average dipole moment $p_z=|Q^{\pm}|\times d_z$ and the value of the potential change. As a function of adsorption site, the estimated size of the surface dipole is found to roughly correlate with the size of the work function change. It is interesting to note that, in spite of there being less charge redistributed for the D site than for the T_2' site, the former site exhibits a longer dipole length, thus explaining the larger potential change for this site.

The above results allow us first to estimate a value for the *macroscopic* electronic charge transfer Δn_e by integrating $\Delta\rho(\mathbf{r})$ within a set of concentric spherical volumes of increasing radius R_c, centered at each Cs atomic position. The resulting integrated charge versus integration radius curves are shown in Fig. 8 for each of the three sites. We show only the contribution from the outermost valence orbital.[49] The value of Δn_e is estimated by considering a characteristic radius of the order of the distance between Cs and the nearest surface atoms (see Table III): this is slightly larger than the

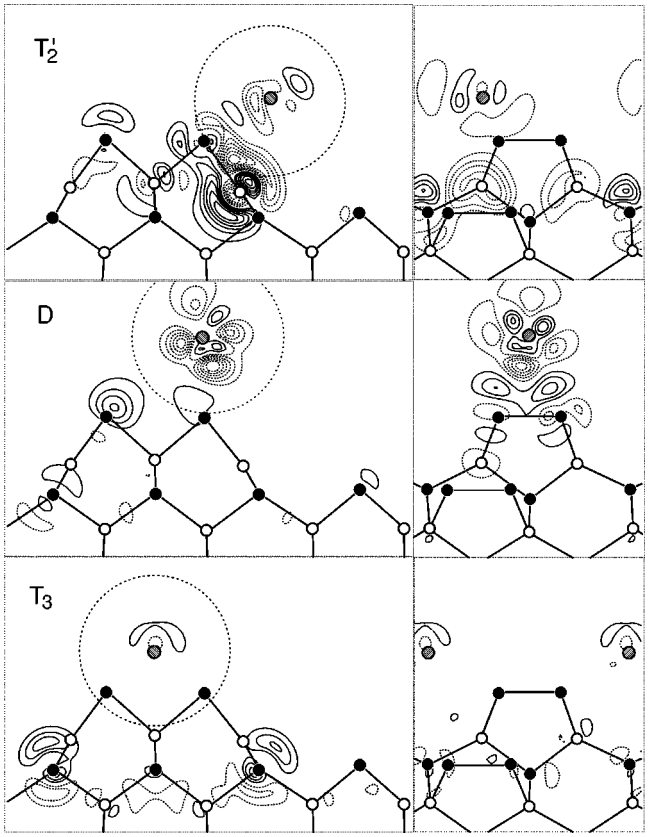

FIG. 9. Charge density difference contour maps for the T_2' (top), D (center), and T_3 (bottom) surfaces. Each figure shows $\Delta\rho(\mathbf{r})$ computed on the planes perpendicular (left column) and parallel (right column) to the $[1\bar{1}0]$ direction that contain the Cs atom position. Solid lines represent electron accumulation regions ($\Delta\rho<0$) and dashed lines electron depletion regions ($\Delta\rho>0$) after adsorption. Contour separation is 0.0014 bohr^{-3} and contours begin at ($\pm$) this value. The Cs atomic sphere (taking a radius of 3 Å) is indicated in each case.

atomic radius of 2.98 Å.[50] We find a significant charge transfer of about $0.75e$ for the T_2' surface, close to the value of $0.7e$ obtained for the cleavage face.[12] Since the corresponding charge transfer occurs to a localized state, simple treatments should allow us to understand its value. Indeed, applying a self-consistent tight-binding model to describe a bond between Cs and the gallium dangling bond,[51,52] we calculate a transferred charge very close to unity. On the other hand, the estimated charge transfer is smaller for D with a value for Δn_e of less than $0.2e$ and even smaller for the T_3 sites. For the D site, the small charge transfer is in agreement with the relatively weak interaction with the nearby $C4$ state of the clean surface, and since $C4$ is partly built from the dimer antibonding state, it reflects that As dimers are weakly affected by adsorption.

The microscopic mechanisms underlying the above results are shown in Fig. 9, which presents cross sections of $\Delta\rho(\mathbf{r})$ along mutually perpendicular planes containing the Cs atom. The function $\Delta\rho(\mathbf{r})$ exhibits positive regions (electron depletion) and negative regions (electron accumulation). Due to the extended nature of the Cs-induced states, the shapes of these regions are more complex than for adsorption at the cleavage face, but they allow us to illustrate elementary mechanisms for dipole formation discussed in the Introduction. For the T_2' site the main feature appears along the Cs-Ga direction and corresponds to a charge depletion inside the atomic sphere and a charge excess outside of it, both of them being localized near the Ga atom close to the Cs. The region of charge excess corresponds to the region of localization of the Cs-induced state described in the preceding subsection, indicating that charge is transferred from the valence s electron of the alkali to the Cs-induced state. This transfer is large enough to cause significant screening processes. The relaxation of the Ga atom induces a smaller dipole, apparent in the contour map in the immediate vicinity of the Ga atom, which has the opposite sign as the transfer-induced one. Other screening dipoles are also present in the vicinity of the alkali and at the top layer dimer atoms.

For the D site, examination of the clouds shows that the charge redistribution, in contrast with the preceding picture, occurs mostly in the region *between* the Cs atom and As dimers. This is a direct consequence of the mixing of the adatom state with the $C4$ state of the clean surface and is similar to the picture valid for adsorption at the cleavage face.[12] Also observed is a smaller electron accumulation above the Cs atom, which reveals some intra-atomic polarization (e.g., $6s$-$6p$ mixing).[53]

For the T_3 site, there is hardly any charge movement within the atomic sphere, which implies that both adatom polarization and charge transfer are minimal. This is in qualitative agreement with the above finding that the Cs-induced dipole is smaller than for the two above sites. The pictures allow us, however, to suggest a substrate polarization, similar to that found by Kobayashi *et al.*[53] for Na and K adsorption on Si(001). This polarization mostly concerns the third-layer As atoms.

V. CONCLUSIONS

In this work, we have studied the geometric and electronic properties of the GaAs(001)$\beta_2(2\times4)/c(2\times8)$ surface under low coverages of cesium. Here, we summarize the main results.

(a) As found from a global analysis of the results, both theoretical and experimental, it seems likely that multiple-site occupation occurs in the early stages of Cs adsorption. It is clear that the choice has to be restricted to three sites, which are the dimer site D, the gallium dangling bond site T_2', and to some minor extent the arsenic T_3 trench site. The T_3 site is found, however, to have the largest adsorption energy, which can be reconciled with the experimental results by taking into consideration the relative areas of the collection basins for the various sites—namely, 1 site/cell for T_3, in contrast with 2 and 4 sites/cell for the D and T_2' sites. No appreciable Cs-induced relaxation and, in particular, no breaking of surface As dimers are observed.

(b) Cs-substrate bonding at the three sites exhibits interesting features and allows us to illustrate two extreme limiting cases on the same surface for the Ga site (T_2') and for the As sites (D and T_3), respectively. At the T_2' site the bonding

is strongly ionic, and is characterized by a relatively large electron transfer, of the order of $0.75e$, to a new Cs-induced state localized behind the second layer Ga atom. Bonding at the other two sites is better described by mixing with existing clean surface states and low charge transfer ($<0.2e$). These site-dependent differences in the charge transfer and net surface dipole lead to site-dependent changes in the work function, for which the *D* site exhibits the largest Cs-induced change.

ACKNOWLEDGMENTS

The upgrading of the surface diffraction station at Lure has been made under EC Contract No. CI1.CT93.0034. C.H. has been supported by the EU through the NANOPHASE Research Training Network (Contract No. HPRM-CT-2002-00167). Computer time was granted by IDRIS (project 544). We acknowledge helpful discussions with Olivia Pulci, R. Natoli, and Rodolfo Del Sole. G.O. acknowledges support of the Italian MIUR-COFIN 2002 and the INFM PAIS CELEX.

[1] G. Vergara, L.J. Gomez, J. Capmany, and M.T. Montojo, Surf. Sci. **131**, 278 (1992).
[2] D. Rodway, Surf. Sci. **103**, 147 (1984).
[3] H. Hamamatsu, H.W. Yeom, T. Yokoyama, T. Kayama, and T. Ohta, Phys. Rev. B **57**, 11 883 (1998).
[4] M. Prietsch, M. Domke, T. Mandel, C. Xue, and G. Kaindl, Z. Phys. B: Condens. Matter **74**, 1989 (1989).
[5] J.A. Martin-Gago, M.C. Asensio, P. Aebi, R. Fasel, D. Naumovic, J. Osterwalder, M.C. Refolio, J.M. Lopez-Sancho, and J. Rubio, Phys. Rev. B **57**, 9201 (1998).
[6] N.J. DiNardo, T.M. Wong, and E.W. Plummer, Phys. Rev. Lett. **65**, 2177 (1990).
[7] K.D. Lee and J. Chung, Phys. Rev. B **55**, 12 906 (1997).
[8] L.J. Whitman, J.A. Stroscio, R.A. Dragoset, and R.J. Celotta, Phys. Rev. Lett. **66**, 1338 (1991).
[9] H.L. Meyerheim, R. Sawitzki, and W. Moritz, Phys. Rev. B **52**, 16 830 (1995), and references therein.
[10] H.L. Meyerheim, N. Jedrecy, M. Sauvage-Simkin, and R. Pinchaux, Phys. Rev. B **58**, 2118 (1998), and references therein.
[11] M.G. Betti, V. Corradini, M. Sauvage-Simkin, and R. Pinchaux, Phys. Rev. B **66**, 085335 (2002).
[12] F. Bechstedt and M. Scheffler, Surf. Sci. Rep. **18**, 145 (1993).
[13] K.M. Song and A.K. Ray, Phys. Rev. B **50**, 14 255 (1994).
[14] H. Ishida and K. Terakura, Phys. Rev. B **40**, 11 519 (1989).
[15] W.M. Mönch, *Semiconductor Surfaces and Interfaces* (Springer, Berlin, 1993), Vol. 26.
[16] P.N. First, R.A. Dragoset, J.A. Stroscio, R.J. Celotta, and R.M. Feenstra, J. Vac. Sci. Technol. A **7**, 2868 (1989).
[17] D.M. Riffe, G.K. Wertheim, J.E. Rowe, and P.H. Citrin, Phys. Rev. B **45**, 3532 (1992).
[18] V.L. Alperovich and D. Paget, Phys. Rev. B **56**, R15 565 (1997).
[19] V. Heine, Phys. Rev. **138**, A1689 (1965).
[20] Y. Garreau, M. Sauvage-Simkin, N. Jedrecy, R. Pinchaux, and M.B. Veron, Phys. Rev. B **54**, 17 638 (1996).
[21] T. Hashizume, Q.K. Xue, J. Zhou, A. Ichimiya, and T. Sakurai, Phys. Rev. Lett. **73**, 2208 (1994).
[22] W.G. Schmidt and F. Bechstedt, Phys. Rev. B **54**, 16 742 (1996).
[23] B. Goldstein, Surf. Sci. **47**, 143 (1975).
[24] J. Kim, M.C. Gallagher, and R.F. Willis, Appl. Surf. Sci. **67**, 286 (1993).
[25] R. Rincon, J. Ortega, F. Flores, A.L. Yeyati, and A. Martin-Rodero, Phys. Rev. B **52**, 16 345 (1995).
[26] C. Hogan, D. Paget, O. E. Tereshchenko, L. Reining, and G. Onida (unpublished).
[27] S.G. Louie, S. Froyen, and M.L. Cohen, Phys. Rev. B **26**, 1738 (1982).
[28] The alternative strategy of including only the 6*s* electron in the valence and using the NLCC scheme (Ref. 27) was also considered, but it was found to yield considerably less satisfactory results.
[29] D.R. Hamann, Phys. Rev. B **40**, 2980 (1989).
[30] D. Vanderbilt, Phys. Rev. B **41**, 7892 (1990).
[31] G.B. Bachelet, D.R. Hamann, and M. Schlüter, Phys. Rev. B **26**, 4199 (1982).
[32] I. Moullet, W. Andreoni, and P. Giannozzi, J. Chem. Phys. **90**, 7306 (1989).
[33] A.R. Miedema and J.W.F. Dorleijn, Surf. Sci. **447**, 95 (1980).
[34] O.E. Tereshchenko, V.S. Voronin, H.E. Scheibler, V.L. Alperovich, and A.S. Terekhov, Surf. Sci. **507–510**, 51 (2002).
[35] M. Domke, T. Mandel, C. Laubschat, M. Prietsch, and G. Kaindl, Surf. Sci. **189/190**, 268 (1987).
[36] E. Vlieg, J. Appl. Crystallogr. **33**, 401 (2000).
[37] Direct comparison between calculated atomic coordinates and experimental data is not straightforward. First, the experimental and theoretical lattice parameters differ by 2%, which forces a comparison of reduced atomic coordinates with respect to the unit cell dimensions. Second, for the clean surface, discrepancies of the order of 10^{-3} exist between the experimental and theoretical reduced coordinates. These differences produce an increase of χ^2_{red} which is not related to Cs adsorption.
[38] J.H. VanVucht, J. Less-Common Met. **109**, 163 (1985).
[39] The experimental surface does not have metallic—i.e., conductive—character, because at low coverage interactions between neighboring Cs are weak and possibly also because of charge transfer to bulk states of the solid as shown in Ref. 40. Our ideal, periodic surface calculation overestimates the strength of these interactions, so that the presence of a partially occupied band does not imply that the surface is electrically conductive.
[40] V.L. Alperovich, A.G. Paulish, and A.S. Terekhov, Phys. Rev. B **50**, 5480 (1994).
[41] M.D. Pashley and K.W. Haberern, Phys. Rev. Lett. **67**, 2697 (1991).
[42] P. Bennich, C. Puglia, P.A. Bruhwiler, A. Nilsson, A.J. Maxwell, A. Sandell, N. Martensson, and P. Rudolf, Phys. Rev. B **59**, 8292 (1999).
[43] The thick vacuum calculations were performed with a thinner substrate (eight layers) due to computational limitations. However, we verified that the electrostatic potential in layers 2–5 matched that of the thick slab to within 0.01 eV.
[44] J. Neugebauer and M. Scheffler, Phys. Rev. B **46**, 16 067 (1992).
[45] A. Baldereschi, S. Baroni, and R. Resta, Phys. Rev. Lett. **61**, 734 (1988).

[46] H. Tsuda and T. Muzutani, Appl. Phys. Lett. **60**, 1570 (1992).
[47] R.H. Miwa and G.P. Srivastava, Phys. Rev. B **62**, 15 778 (2000).
[48] The present calculation (one Cs atom per unit cell) corresponds to a coverage of 12% of the number of substrate atoms, whereas experimental coverages are rather expressed as a function of saturation coverage θ_{sat}, which is known to approximately correspond with the concentration of substrate atoms (Refs. 1 and 2).
[49] Integration over the other eight electrons ($5s^2 5p^6$) which we have defined to be valence electrons is completed at a radius $R_c = 2.01$ Å for the Cs atom, in good agreement with literature values for the ionic radius of Cs. Note that, since about $0.11e$ is found to lie outside the largest sphere which can be inscribed in the supercell, we have normalized the vertical axis such that at the cell edge, $n_e = 9.0e$ precisely.
[50] Values taken from http://www.webelements.com, and references therein.
[51] I. Lefebvre, M. Lannoo, and G. Allan, Europhys. Lett. **10**, 359 (1989).
[52] M. Lannoo and P. Friedel, *Atomic and Electronic Surface States* (Springer, Berlin, 1991), Vol. 2.
[53] K. Kobayashi, Y. Morikawa, K. Terakura, and S. Blügel, Phys. Rev. B **45**, 3469 (1992).